Nanoscale

Esterase- and pH-responsive poly(beta-amino ester)-capped mesoporous silica nanoparticles for drug delivery

Journal:	*Nanoscale*
Manuscript ID:	NR-COM-12-2014-007443.R1
Article Type:	Communication
Date Submitted by the Author:	25-Feb-2015

Complete List of Authors:	Fernando, Isurika; Northwestern University, Chemistry Ferris, Daniel; Northwestern University, Chemistry Frasconi, Marco; Northwestern University, Chemistry Malin, Dmitry; University of Wisconsin, Medicine and Public Health Strekalova, Elena; University of Wisconsin, Medicine and Public Health Yilmaz, M. Deniz; Northwestern University, Chemistry Ambrogio, Michael; Nortwestern University, Atomic and Nanoscale Characterization and Experimental (NUANCE) Center Algaradah, Mohammed; Joint Center of Excellence in Integrated Nano-Systems, Kind Abdul-Aziz City for Science and Technology Hong, Michael; Northwestern University, Department of Chemistry Chen, Xinqi; Nortwestern University, Atomic and Nanoscale Characterization and Experimental (NUANCE) Center Botros, Youssry; University Research Ofiice, Intel Corporation, Nassar, Majed; King Abdulaziz City of Science and Technology, National Center for Nano Technology Research, Cryns, VL; University of Wisconsin, Medicine and Public Health Stoddart, J.; Northwestern University, Chemistry

Nanoscale

Esterase- and pH-responsive poly(β-amino ester)-capped mesoporous silica nanoparticles for drug delivery†

Isurika R. Fernando,[a] Daniel P. Ferris,[a] Marco Frasconi,[a] Dmitry Malin,[b] Elena Strekalova,[b] M. Deniz Yilmaz,[a] Michael W. Ambrogio,[c] Mohammed M. Algaradah,[d] Michael P. Hong,[a] Xinqi Chen,[c] Majed S. Nassar,[d] Youssry Y. Botros,[d,e] Vincent L. Cryns,*[b] and J. Fraser Stoddart*[a]

[a]Department of Chemistry, Northwestern University
2145 Sheridan Road, Evanston, IL 60208, USA
E-mail: stoddart@northwestern.edu

[b]Department of Medicine, University of Wisconsin Carbon Cancer Center
University of Wisconsin School of Medicine and Public Health
3018 WIMR, 1111 Highland Avenue, Madison, WI 53705, USA
E-mail: vlcryns@medicine.wisc.edu

[c]Northwestern University Atomic and Nanoscale Characterisation and Experimental (NU*ANCE*) Center
Northwestern University, 2220 Campus Drive, Evanston, IL 60208, USA

[d]Joint Center of Excellence in Integrated Nano-Systems (JCIN)
King Abdul-Aziz City for Science and Technology (KACST)
P.O. Box 6086, Riyadh 11442, Kingdom of Saudi Arabia

[e]University Research Office, Intel Corporation, Building RNB-6-61
2200 Mission College Boulevard, Santa Clara, CA 95054, USA

Gating of mesoporous silica nano particles (MSNs) with the stimuli responsive poly(*β*-amino ester) has been achieved. This hybrid nanocarrier releases doxorubicin (DOX) under acidic conditions or in the presence of porcine liver esterase. The DOX loaded poly(*β*-amino ester)-capped MSNs lower the cell viability when tested on MDA-MB-231 human breast cancer cells.

Serious side-effects that arise because of the nonspecific cell / tissue bio-distribution[1] of cytotoxic anticancer therapeutic agents constitute one of the fundamental drawbacks of conventional chemotherapy. Consequently, drug encapsulation has emerged as a promising strategy to reduce the side-effects of these agents by instituting, controlled release of the drug on demand.[2] Surface-functionalised, end-capped mesoporous silica nanoparticles (MSNs) have received[3] much attention during the past decade because of their potential applications in the stimuli-responsive, controlled release of drugs and genes. Proof of concept experiments involving a wide variety of responsive stimuli have been explored.[3,4] Cancer cells are extremely biodiverse, however, and have very different intracellular biochemical environments based on protein expression.[5] Hence, it is important to design materials that can respond to many of the biochemical abnormalities of cancer cells, while maintaining high tolerability toward the organism as a whole. For these reasons, we set out to investigate multifunctional systems with distinct similarities in design to clinically approved protocols.

Although a large number of capping agents such as small molecules, supramolecular nanovalves, and polymers have been reported[3,4] to act as stimuli responsive nanogates on MSN drug delivery vehicles, the capping of MSNs with polymers (i) has potential to address biomedical applications, (ii) has seen an ever increasing literature[6] interest and (iii) has many still yet unexplored areas of research. Moreover, a large number of materials currently used for clinical

research are themselves biocompatible polymers.[7] Therefore, by hybridising these two – polymers and MSNs – we stand to gain the benefits of each component. Poly(ethylene glycol) (PEG),[6b,d,g,h,j] poly(methacrylic acid) (PMAA),[6c] *N*-isopropylacrylamide (NIPAM),[6c-e] poly(glycidyl methacrylates) (PGMAs)[6k-n] and poly(acrylic acid) (PAA)[6a] have been used as pH,[6a,c,e,g,k,m,n] temperature,[6c,d,g] UV-Vis[6f,h,l] and near IR[6i] stimuli-triggered polymer-end-caps for the controlled release of drugs from the pores of MSNs.[5] It shows that activation of currently available hybrid MSN-polymer systems to release drugs requires an external physical stimuli with the proviso that they do not respond to the biochemical machinery within the cells with the exception of pH- triggered[6a,c,e,g,k,m,n] drug release.

Poly(*β*-amino esters)[8] constitute a class of polymers which, to our knowledge, have never been used as caps for MSNs. They captured our attention, because of their biocompatibility, together with the fact that (i) they can be prepared from relatively inexpensive starting materials, (ii) there exists a feasible protocol for their synthesis and purification. The ease with which synthetic modifications can be carried out on them so that they can acquire a range of different physical and chemical properties[8] also renders them attractive. In cancer therapy, acidic response has been explored widely as a stimulus in order to detach the end-caps of MSN drug delivery vehicles[9] based on the pH difference between normal tissue and the bloodstream (pH 7.4), and the extracellular environment surrounding cancerous cell tissue (pH 6.0–7.0). In cancer cells, the pH drops[10] even moreso inside the endosomal (pH 5.5–6.0) and the lysosomal (pH 4.5–5.0) compartments. Also, it is generally accepted that the cytosol in the cancer cells contains esterase concentrations that are two to three orders of magnitude higher than those in the extracellular fluid.[11] Add into the equation the fact that boronic acids are a class of compounds which undergo facile boronate ester formation with *cis*-diols and the fact that the resulting cyclic esters are

highly sensitive to the pH of the medium[12] and we have a good combination of design criteria for end-capping MSN drug delivery vehicles.

Consequently, we decided to marry the advantages of the pH sensitivity of the boronate esters with the ease of modifying poly(*β*-amino esters) synthetically to gather together the beneficial properties from both sides. Herein, we report on the development of a esterase- and pH-responsive poly(*β*-amino ester)-capped MSN (POL-MSN) integrated system as a controlled drug delivery vehicle. Modification of the main chain of the polymer with ester functions facilitates the cleavage of the polymer by esterases. Furthermore, incorporation of catechol as a side chain along the polymer backbone, while covering the MSNs with phenyl boronic acid, assists (Fig. 1) the capping of MSNs by boronate ester bond formation and hence traps the cargos inside the mesopores of MSNs. In this manner, polymer-capped MSNs reap the benefits of the chemical abnormalities in cancer cells – namely, low pH and high esterase concentrations – to bring about the detachment synergistically of the polymer caps and the release of the cargos from these 'smart' nanomaterials into the cellular environment of diseased cells. We believe that this approach has considerable advantages to offer in cancer therapy over the singly stimuli-responsive systems.

In order to evaluate the release of cargo from this dual-activation system, we employed two different cargos – namely, the fluorescent dye, propidium iodide (PI) and the anticancer drug, doxorubicin (DOX). Preliminary pH- and esterase-triggered solution studies were carried out exclusively with PI as the loaded cargo so as to determine the patterns associated with its controlled release. We have also shown that these cargo-loaded polymer-capped nanomaterials can be taken up by MDA-MB-231 human breast cancer cells prior to the release of the cargo

from the uncapped MSN. In these experiments, we have demonstrated the potential of POL-DOX-MSNs as efficient and effective nanocarriers to deliver drugs to MBA-MD-231 breast cancer cells.

The catechol derivative of poly(*β*-amino ester) was prepared (Fig. 2) using a Michael addition. Reaction of triethylene glycol diacrylate with dopamine hydrochloride in the presence of NEt_3 yielded POL. Gel permeation chromatography (GPC) and ^{1}H NMR spectroscopy were used to characterise the POL. See ***Section 2.2*** of the ESI.

The synthesis of MCM-41 nanoparticles, followed by surface modification was carried out according to modified literature procedures.[13] MCM-41-type MSNs, with average particle size diameters of *ca*. 100 nm and pore diameters of *ca*. 2 nm, were prepared by traditional base-catalysed, sol-gel protocols in the presence of cetyl trimethyl ammonium bromide (CTAB) as the nanoporous template. The CTAB template was removed from the particles by multiple extractions with acidic MeOH. 3-Aminopropyltriethoxysilane was condensed on the surfaces of MSNs in order to introduce amino functional groups, affording AP-MSNs. Boronic acids were assembled on to the surface of the nanoparticles to give PBA-MSNs by carrying out a condensation between 4-carboxy-3-fluorophenylboronic acid and the AP-MSNs. The constitutions and the surface properties of all these nanomaterials were characterised at each stage in their preparation by calling upon a wide array of analytical techniques, including (i) powder X-ray diffraction (PXRD), (ii) N_2 adsorption and desorption isotherms, (iii) transmission electron microscopy (TEM), (iv) scanning electron microscopy (SEM), (v) ζ potential measurements, (vi) X-ray photoelectron spectroscopy (XPS), (vii) Fourier transform infrared

(FT-IR) spectroscopy and (viii) time-of-flight secondary ion mass spectrometry (ToF-SIMS). See ***Section 4*** of the ESI.

Once the PBA-MSNs had been prepared and fully characterised, drug-loading, followed by capping, was carried out (Fig. 1) in solution in order to construct the hybrid drug nanocarriers. The mesopores of PBA-MSNs were loaded with PI (4 mg / 1 mL) or DOX (1 mg / 1 mL) in pH 7.4 phosphate-buffered saline (PBS) (1 mL / 10 mg of PBA-MSN). Since DOX has a greater fluorescence quantum yield than PI, relatively lower concentrations of DOX and higher concentrations of PI were employed in the drug-loading step. After 24 h of cargo loading at room temperature, an aqueous solution of the polymer (PBA-MSN : POL = 1 : 2, w/w) in trace amounts of Me_2SO was added to the mixture. Reversible covalent bond formation at pH 7.4 between the phenyl boronic acid residues anchored onto the PBA-MSN and the catechol-containing side chains of the POL encapsulate the cargo molecules inside the mesopores of the MSNs as a result of the formation of a string of cyclic boronate esters. When the nanoparticles were loaded with PI, this protocol yielded poly(*β*-amino ester) capped, PI-loaded mesoporous silica nanoparticles (POL-PI-MSNs). Alternatively, when the nanoparticles were loaded with DOX, poly(*β*-amino ester)-capped, doxorubicin-loaded mesoporous silica nanoparticles (POL-DOX-MSNs) were isolated.

The pH- or esterase-triggered cargo release was monitored (Fig. S10†) using fluorescence emission spectroscopy. The POL-PI-MSNs or POL-DOX-MSNs were placed in the corner of a quartz cuvette and it was filled up with the PBS buffer (pH 7.4). The resulting mixture was stirred slowly so as to accelerate the dispersion of the released cargo without disturbing the nanoparticles. After applying the stimulus/stimuli, dissociation of the caps followed by

unloading of the cargo, was monitored by exciting the dissolved cargo molecules – either PI ($\lambda_{excitation}$ = 500 nm) or DOX ($\lambda_{excitation}$ = 480 nm) – in the solution. The fluorescence emission spectra were recorded every 10 min for the first 2 hours and then every 30 min thereafter. Release % of DOX and PI were calculated using fluorescence calibration plots of DOX and PI along with the fluorescence emission spectra. Plots of time versus release % constitute the release profiles (Fig. 3) for the cargos.

The pH-triggered cargo release profiles were monitored after adjusting the pH of the solution to the desired value with a dilute HCl solution. The release profile of PI at pH 7.4 revealed (Fig. 3a) insignificant premature release of cargo during the course of experiment, indicating that the phenyl boronate esters are stable at physiological pH. Cargo release as the solution is acidified demonstrates that the boronate esters are no longer stable and the outcome of their cleavage is the uncapping of the polymer from the MSNs. Free of steric inhibition at the mesopore openings, the loaded cargo is able to diffuse out of the MSNs. The release profile of PI at pH 4.0 shows by far the highest release kinetics which decrease gradually at pH 5.0 and 6.0. This observation can be attributed to the cleavage of a large percentage of boronate ester bonds, followed by uncapping and the physical release of the cargo from the mesopores of the MSNs. Interestingly, under all the acidic pH conditions investigated, release profiles of PI reach a plateau inside 2 hours, indicating the release of cargo has reached equilibrium. This 2-hour window is highly beneficial for drug delivery since the ‘smart’ nanomaterials unload all the cargo before the nanoparticles are exocytosed and provide a larger cargo burst that can help to increase the particle efficacy of drug-loaded nanoparticles.

The esterase responsive release of cargo from the hybrid nanomaterials was carried out using a typical delivery experiment, similar to that described already for pH-triggered cargo release.

Instead of HCl, esterase was employed as the trigger which was introduced as a solution of esterase that was prepared by dissolving the enzyme (1.0 mg) in pH 7.4 PBS buffer (0.5 mL). The esterase-responsive release profiles (Fig. 3b) of POL-PI-MSN demonstrate that this biological catalyst, cleaves the POL and releases the PI, indicating ester groups in the backbone of the polymer that have been hydrolysed enzymatically. Additionally, the cargo release profile reaches a plateau within 2 hours, showing that esterase-triggered cargo release is competitive with the pH-triggered release.

With rapid expulsion of PI from capped and loaded MSNs in the presence of pH- and esterase-triggers established, we turned our attention to evaluating the behavior of DOX in POL-DOX-MSN nanocarriers, before carrying out cell viability studies. The pH- and esterase-triggered release profiles (Fig. 3c and 3d, respectively) of DOX confirm that the POL-DOX-MSN drug delivery vehicles follow the same of polymer-uncapping and the cargo release as true POL-PI-MSNs.

When the pH-triggered release profile at pH 4.0 reaches (Fig. 3a and 3c) the release equilibrium, approximately 0.12 μmol of PI and 0.02 μmol of DOX are released from 3.5 mg of POL-PI-MSNs and 1.0 mg of POL-DOX-MSNs, respectively. The amount of released PI corresponds to a 2.6 % release capacity while it is 2.4 % for DOX. These release capacities correspond to the release efficiencies of 83 % and 85% for PI and DOX, respectively. When the esterase-triggered release profile reaches (Fig. 3b and 3d) a plateau, approximately 0.10 μmol of PI and 0.015 μmol of DOX are released from the corresponding drug-loaded nanomaterials which equate with the 2.4 and 2.2 % release capacities of PI and DOX, respectively. These release capacities correspond to the release efficiencies of 71 % for PI and 77 % for DOX. In order to determine

the dose for *in vitro* cell studies, these release capacities were taken in to the account. See ***Section 7*** of the ESI for further information, particularly Tables S2 and S3.

With the chemical characterisation and release mechanism of the cargo delivery vehicles in solution well understood, POL-PI-MSNs were subjected to cellular internalisation experiments in order to track the localisation of the MSNs in MDA-MB-231 human breast cancer cells as a prelude to using POL-DOX-MSNs to evaluate its possible therapeutic applications. The cellular uptake of POL-PI-MSNs and POL-PI-FITC-MSNs was investigated using fluorescence microscopy. Photomicrographs of MDA-MB-231 breast cancer cells show (Fig. S11†) that the nanomaterials are taken up by the cells since the released PI stains the nucleus and exhibits the red emission of PI on excitation at 500 nm.

Cell viability tests were performed (Fig. 4) on MDA-MB-231 breast cancer cells in order to evaluate the cytotoxicity of the vehicle (pH 7.4 PBS buffer), PBA-MSNs, POL-MSNs and DOX itself as control experiments against the POL-DOX-MSNs. The detailed procedure for the crystal violet cell-survival assay is presented in the ***Section 9*** of ESI.[14] Briefly, after treating MDA-MB-231 breast cancer cells with the nanomaterials for 96 hours, the cells were washed with pH 7.4 PBS buffer and the surviving cells were stained with crystal violet. The vehicle and PBA-MSNs resulted in insignificant cytotoxicity against MDA-MB-231 breast cancer cells, while the POL-MSNs resulted in modest cytotoxicity under these conditions (Fig. 4a–c). In order to provide the same dose of DOX, the breast cancer cells were treated with either 2 μg/ml of free DOX as the control or 64 μg/ml of POL-DOX-MSNs, which release 2 μg/ml DOX at pH 5.5. Optical microscopy images of DOX and POL-DOX-MSNs treated cells reveal (Fig. 4d and 4e) that the POL-DOX-MSNs have a similar cytotoxicity as the same dose of free DOX. This finding can

likely be attributed to the cleavage of the polymer cap and the release of DOX from the mesopores of the MSNs as a consequence of the synergistic effect of acidic pH and the high concentration of esterase present in the cancer cells. The cell confluence plot (Fig. 4f) summarizes the cell viability data and confirms that POL-DOX-MSNs induce cell death of MDA-MB-231 breast cancer cells.

In summary, we have designed and synthesised a poly(*β*-amino ester) cap for MSNs and demonstrated that the POL-capped MSNs can serve as 'smart' nanomaterials for esterase- and pH-triggered controlled release of anticancer drugs and exert robust cytotoxic effects against MDA-MB-231 human breast cancer cells. With the objective of adapting this smart nanocarrier for *in vitro* and *in vivo* drug delivery, we envision this system responding to a wider spectrum of cell physiologies observed within cancer biodiversity.

Acknowledgements

This research is part (Project 34-941) of the Joint Center of Excellence in Integrated Nano-Systems (JCIN) at King Abdul-Aziz City for Science and Technology (KACST) and Northwestern University (NU). The authors would like to thank both KACST and NU for their continued support of this research.

†Electronic Supplementary Information (ESI) available: Experimental details relating to (i) the synthesis and characterisation of the surface-functionalised MSN and POL (ii) cargo-loading and release studies in solution, (iii) cellular internalisation of nanomaterials, and (iv) cell viability tests are available in the Electronic Supplementary Information.

Received: ((will be filled in by the editorial staff))

Accepted: ((will be filled in by the editorial staff))

First published online: ((will be filled in by the editorial staff))

Notes and References

1 R. T. Skeel and S. N. Khleif, *Handbook of Cancer Chemotherapy*, Lippincott Williams & Wilkins, Philadelphia, 8th edn., 2011, pp 1–15 and 45–62.

2 (*a*) D. Peer, J. M. Karp, S. Hong, O. C. Farokhzad, R. Margalit and R. Langer, *Nature Nanotech.*, 2007, **2**, 751–760; (*b*) O. C. Farokhzad and R. Langer, *ACS Nano*, 2009, **3**, 16–20; (*c*) H. Meng, M. Xue, T. Xia, Z. Ji, D. Y. Tran, J. I. Zink and A. E. Nel, *ACS Nano*, 2011, **5**, 4131–4144; (*d*) A. A. Alexander-Bryant, W. S. Vanden Berg-Foels and X. Wen, *Adv. Cancer Res.* 2013, **118**, 1–59; (*e*) S. Nazir, T. Hussain, A. Ayub, U. Rashid and A. J. MacRobert, *Nanomedicine*, 2014, **10**, 19–34; (*f*) J. Kroon, J. M. Metselaar, G. Storm and G. van der Pluijm, *Cancer Treat. Rev.*, 2014, **40**, 578–584.

3 (*a*) A. B. Descalzo, R. Martínez-Máñez, F. Sancenón, K. Hoffmann and K. Rurack, *Angew. Chem. Int. Ed.*, 2006, **45**, 5924–5948; (*b*) I. I. Slowing, B. G. Trewyn, S. Giri, V. S.-Y. Lin, *Adv. Funct. Mater.*, 2007, **17**, 1225–1236; (*c*) K. K. Coti, M. E. Belowich, M. Liong, M. W. Ambrogio, Y. A. Lau, H. A. Khatib, J. I. Zink, N. M. Khashab and J. F. Stoddart, *Nanoscale*, 2009, **1**, 16–39; (*d*) J. M. Rosenholm, C. Sahlgren and M. Lindén, *Nanoscale*, 2010, **2,** 1870–1883; (*e*) J. L. Vivero-Escoto, I. I. Slowing, B. G. Trewyn and V. S.-Y. Lin, *Small*, 2010, **6**, 1952–1967; (*f*) M. W. Ambrogio, C. R. Thomas, Y.-L. Zhao, J. I. Zink and J. F. Stoddart, *Acc. Chem. Res.*, 2011, **44**, 903–913; (*g*) Z. Li, J. C. Barnes, A. Bosoy, J. F. Stoddart and J. I. Zink, *Chem. Soc. Rev.*, 2012, **41**, 2590–2605; (*h*) M. Vallet-Regí, M. Manzano García and M. Colilla, *Biomedical Applications of Mesoporous Ceramics: Drug Delivery, Smart Materials and Bone Tissue Engineering*, CRC Press, 2012, pp 1–231; (*i*) C. Coll, A. Bernardos, R. Martínez-Máñez and F. Sancenón, *Acc. Chem. Res.*, 2013, **46**, 339–349; (*j*) D. Tarn, C. E. Ashley, M. Xiu, E. C. Carnes, J. I. Zink and C. J. Brinker, *Acc. Chem. Res.*, 2013, **46**, 792–801; (*k*) C. Argyo, V. Weiss, C. Braüchle and T. Bein, *Chem. Mater.*, 2014, **26**, 435–451; (*l*) M. Vallet-Regí, *Bioceramics with Clinical Applications*, John Wiley & Sons Inc., 2014, pp 109–151, 343–382 and 421–455; (*m*) Y.-W. Yang, Y.-L. Sun, N. Song, *Acc. Chem. Res.*, 2014, **47**, 1950–1960.

4 (*a*) S. Angelos, Y.-W. Yang, K. Patel, J. F. Stoddart and J. I. Zink, *Angew. Chem. Int. Ed.*, 2008, **47**, 2222–2226; (*b*) S. Angelos, N. M. Khashab, Y.-W. Yang, A. Trabolsi, H. A. Khatib, J. F. Stoddart, J. I. Zink, *J. Am. Chem. Soc.*, 2009, **131**, 12912–12914; (*c*) S. Angelos, Y.-W. Yang, N. M. Khashab, J. F. Stoddart, J. I. Zink, *J. Am. Chem. Soc.*, 2009, **131**, 11344–11346; (*d*) Y.-W. Yang, *Med. Chem. Commun.*, 2011, **2**, 1033–1049; (*e*) P. Yang, S. Gai and J. Lin, *Chem. Soc. Rev.*, 2012, **41**, 3679–3698; (*f*) Y.-L. Sun, B.-J. Yang, S. X.-A. Zhang, Y.-W. Yang, C*hem. Eur. J.*, 2012, **18**, 9212–9216; (*g*) S. A. Mackowiak, A. Schmidt, V. Weiss, C. Argyo, C. von Schirnding, T. Bein and C. Braeüchle, *Nano Lett.*, 2013, **13**, 2576–2583; (*h*) Y.-L. Sun, Y.-W. Yang, D.-X. Chen, G. Wang, Y. Zhou, C.-Y. Wang and J. F. Stoddart, *Small*, 2013, **9**, 3224–3229; *(i)* R. Villalonga, P. Díez, A. Sánchez, E. Aznar, R. Martínez-

Máñez and J. M. Pingarrón, *Chem. Eur. J.*, 2013, **19**, 7889–7894; (*j*) M. Frasconi, Z. Liu, J. Lei, Y. Wu, E. Strekalova, D. Malin, M. W. Ambrogio, X. Chen, Y. Y. Botros, V. L. Cryns, J.-P. Sauvage and J. F. Stoddart, *J. Am. Chem. Soc.*, 2013, **135**, 11603–11613; (*k*) M. W. Ambrogio, M. Frasconi, Y. D. Yilmaz and X. Chen, *Langmuir*, 2013, **29**, 15386–15393; (*l*) H. Li, L.-L. Tan, P. Jia, Q.-L. Li, Y.-L. Sun, J. Zhang, Y.-Q. Ning, J. Yu, Y.-W. Yang, *Chem. Sci.*, 2014, **5**, 2804–2808; (*m*) Y. Zhou, L.-L. Tan, Q.-L. Li, X.-L. Qiu, A.-D. Qi, Y. Tao, Y.-W. Yang, *Chem. Eur. J.*, 2014, **20**, 2998–3004; (*n*) D. Tarn, D. P. Ferris, J. C. Barnes, M. W. Ambrogio, J. F. Stoddart and J. I. Zink, *Nanoscale*, 2014, **6**, 3335–3343; (*o*) M. D. Yilmaz, M. Xue, M. W. Ambrogio, O. Buyukcakir, Y. Wu, M. Frasconi, X. Chen, M. S. Nassar, J. F. Stoddart and J. I. Zink, *Nanoscale*, 2015, **7**, 1067**–**1072. .

5 R. W. Ruddon, *Cancer Biology*, 8th edn., Oxford University Press, **2007**, pp 105.

6 (*a*) Y. Zhu, J. Shi, W. Shen, X. Dong, J. Feng, M. Ruan and Y. Li, *Angew. Chem. Int. Ed.*, 2005, **44**, 5083–5087. (*b*) V. Cauda, C. Argyo and T. Bein, *J. Mater. Chem.*, 2010, **20**, 8693–8699; (*c*) B. Chang, X. Sha, J. Guo, Y. Jiao, C. Wang and W. Yang, *J. Mater. Chem.*, 2011, **21**, 9239–9247. (*d*) N. Singh, A. Karambelkar, L. Gu, K. Lin, J. S. Miller, C. S. Chen, M. J. Sailor and S. N. Bhatia, *J. Am. Chem. Soc.*, 2011, **133**, 19582–19585; (*e*) L. Sun, X. Zhang, C. Zheng, Z. Wu and C. Li, *J. Phys. Chem. B*, 2013, **117**, 3852–3860; (*f*) X. Wan, T. Liu, J. Hu and S. Liu, *Macromol. Rapid Commun*., 2013, **34**, 341–347; (*g*) B. Chang, D. Chen, Y. Wang Y. Chen, Y. Jiao, X. Sha and W. Yang, *Chem. Mater.*, 2013, **25**, 574–585; (*h*) C. Li, D. Yang, P. Ma, Y. Chen, Y. Wu, Z. Hou, Y. Dai, J. Zhao, C. Sui and J. Lin, *Small*, 2013, **9**, 4150–4159; (*h*) S. Yang, N. Li, D. Chen, X. Qi, Y. Xu, Y. Xu, Q. Xu, H. Li and J. Lu, *J. Mater. Chem. B*, 2013, **1**, 4628–4636; (*i*) W. Ji, N. Li, D. Chen, X. Qi, W. Sha, Y. Jiao, Q. Xu and J. Lu, *J. Mater. Chem. B*, 2013, **1**, 5942–5949; (*j*) J. Dog, M. Xue andJ. I. Zink, *Nanoscale*, 2013, **5**, 10300–10306; (*k*) Y. Sun, Y.-L. Sun, L. Wang, J. Ma, Y.-W. Yang, H. Gao, *Micropor. Mesopor. Mater.*, 2014, **185**, 245-253; (*l*) Q.-L. Li, L. Wang, X.-L. Qiu, Y.-L. Sun, P.-X. Wang,Y. Liu, F. Li, A.-D. Qi, H. Gao, Y.-W. Yang, *Polym. Chem.*, 2014, **5**, 3389–3395; (*m*) Q.-L. Li, Y. Sun,Y.-L. Sun, J. Wen, Y. Zhou,Q.-M. Bing, L. D. Isaacs, Y. Jin, H. Gao and Y.-W. Yang, *Chem. Mater.*, 2014, **26**, 6418–6431; (*n*) Q.-L. Li, W.-X. Gu, H. Gao and Y.-W. Yang, *Chem. Commun.*, 2014, **50**, 13201–13215

7 (*a*) H. Liu, E. B. Slamovich and T. J. Webster, *Int. J. Nanomedicine*, 2006, **1**, 541–545; (*b*) E. Marin, M. I. Briceno and C. Caballero-George, *Int. J. Nanomedicine*, 2013, **8**, 3071–3090.

8 (*a*) D. M. Lynn and R. Lagner, *J. Am. Chem. Soc.*, 2000, **122**, 10761–10768; (*b*) D. M. Lynn, D. G. Anderson, D. Putnam and R. Langer, *J. Am. Chem. Soc.*, 2001, **123**, 8155–8156; (c) J. J. Green, J. Shi, E. Chiu, E. S. Leshchiner, R. Langer and D. G. Anderson, *Bioconjugate Chem.*, 2006, **17**, 1162–1169; (*d*) J. J. Green, R. Langer, D. G. Anderson, *Acc. Chem. Res.*, 2008, **41**, 749–759; (*e*) J. J. Green, G. T. Zugates, R. Langer, D. G. Anderson; *Methods in Mol. Biol.*, 2009, Vol *480*, pp 53–63; (*f*) Y. Zhang, R. Wang, Y. Hua, R. Baumgartner, J. Cheng, *ACS Macro Lett.*, 2014, **3**, 693–697.

9 K.-N. Yang, C.-Q. Zhang, W. Wang, P. C. Wang, J.-P. Zhou and X.-J. Liang, *Cancer Biol. Med.*, 2014, **11**, 34–43.

10 (*a*) I. Mellman, R. Fuchs and A. Helenius, *Annu. Rev. Biochem.*,1986, *55*, 663–700; (*b*) I. F. Tannock and D. Rotin, *Cancer Res.*, 1989, **49**, 4373–4384; (*c*) R. J. Gillies, N. Raghunand, M. L. Garcia-Martin and R. A. Gatenby, *IEEE Eng. Med. Biol. Mag.*, 2004, **23**, 57–64; (*e*) N. Fahrenbacher, M. Jäättelä, *Cancer Res*., 2005, **65**, 2993–2995.

11 (*a*) R. B. Cohen, M. M. Nachlas and A. M. Selingman, *Cancer Res*., 1951, **11**, 709–711; (*b*) B. Monis and T. Weinberg, *Cancer*, 1961, **14**, 369–377; (*c*) O. V. Deimling and A. Böcking, *Histochem. J.*, 1976, **8**, 215–252; (*d*) P. C. Rodriguez, D. G. Quiceno, J. Zabaleta, B. Ortiz, A. H. Zea, M. B. Piazuelo, A. Delgado, P. Correa, J. Brayer, E. M. Sotomayor, S. Antonia, J. B. Ochoa and A. C. Ochoa, *Cancer Res.*, 2004, **64**, 5839–5849; (*e*) K. Patel, S. Angelos, W. R. Dichtel, A. Coskun, Y.-W. Yang, J. I. Zink and J. F. Stoddart, *J. Am. Chem. Soc.*, 2008, **130**, 2382–2383; (*f*) Y.-L. Sun, Y. Zhou, Q.-L. Li, Y.-W. Yang, *Chem. Commun.*, 2013, **49**, 9033–9035.

12 (*a*) T. D. James, K. R. A. S. Sandanayake and S. Shinkai, *Angew. Chem. Int. Ed. Engl.*, 1996, **35**, 1911–1912; (*b*) G. Springsteen and B. Wang, *Tetrahedron*, 2002, **58**, 5291–5300; (*i*) E. Shoji and M. S. Freund, *J. Am. Chem. Soc.*, 2002, **124**, 12486–12493.

13 (*a*) C. T. Kresge, M. E. Leonowicz, W. J. Roth, J. C. Vartuli and J. S. Beck, *Nature*, 1992, **359**, 710–712; (b) Y. Zhao, B. G. Trewyn, I. I. Slowing and V. S.-Y. Lin, *J. Am. Chem. Soc.*, 2009, **131**, 8398–8400.

14 M. Lu, A. Strohecker, F. Chen, T. Kwan, J. Bosman, V. C. Jordan and V. L. Cryns, *Clin. Cancer Res.*, 2008, **14**, 3168–3176.

Captions to Figures

Fig. 1. Schematic representation of (i) cargo loading, (ii) polymer capping and (iii) pH- and esterase-triggered cargo release from mesoporous silica nanoparticles (MSNs)

Fig. 2. Schematics of synthesis of poly(*β*-amino ester) from triethylene glycol diacrylate and dopamine using the Michael addition

Fig. 3. a) pH and b) enzyme-responsive PI release, and c) pH and d) enzyme-responsive DOX release from POL-MSN pores

Fig. 4. Representative optical microscopy images of the crystal violet cell survival assay of MDA-MB-231 breast cancer cells treated with a) the vehicle (PBS pH 7.4), b) POL-MSNs, c) PBA-MSNs, d) DOX or e) DOX-POL-MSNs for 96 hours, and f) the effects of these agents on % cell confluence. **P <0.01, ***P < 0.001 versus vehicle control.

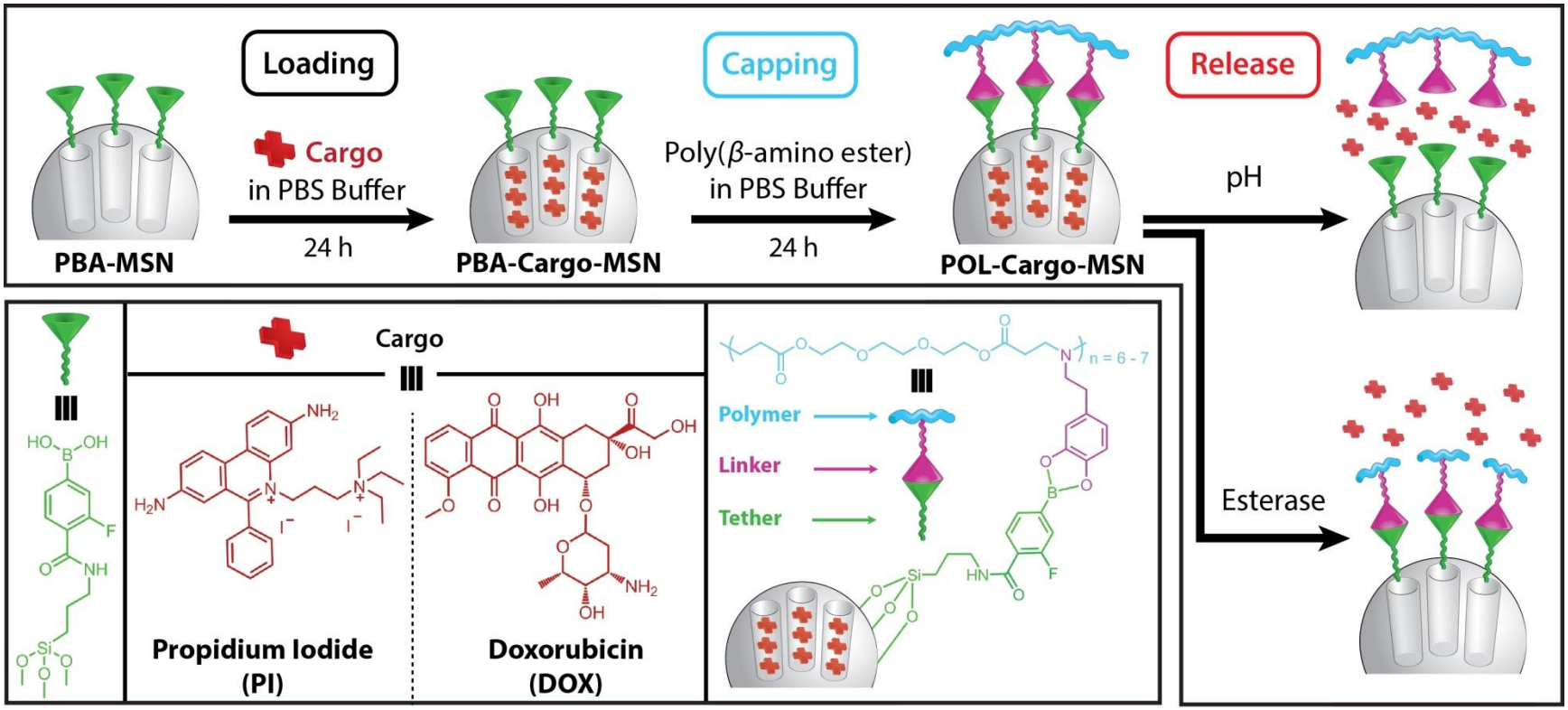
Loading
Cargo
in PBS Buffer
24 h
PBA-MSN
PBA-Cargo-MSN
Capping
Poly(β-amino ester)
in PBS Buffer
24 h
POL-Cargo-MSN
Release
pH
Esterase
Cargo
Propidium Iodide
(PI)
Doxorubicin
(DOX)
Polymer
Linker
Tether
n = 6 - 7

Fig. 1

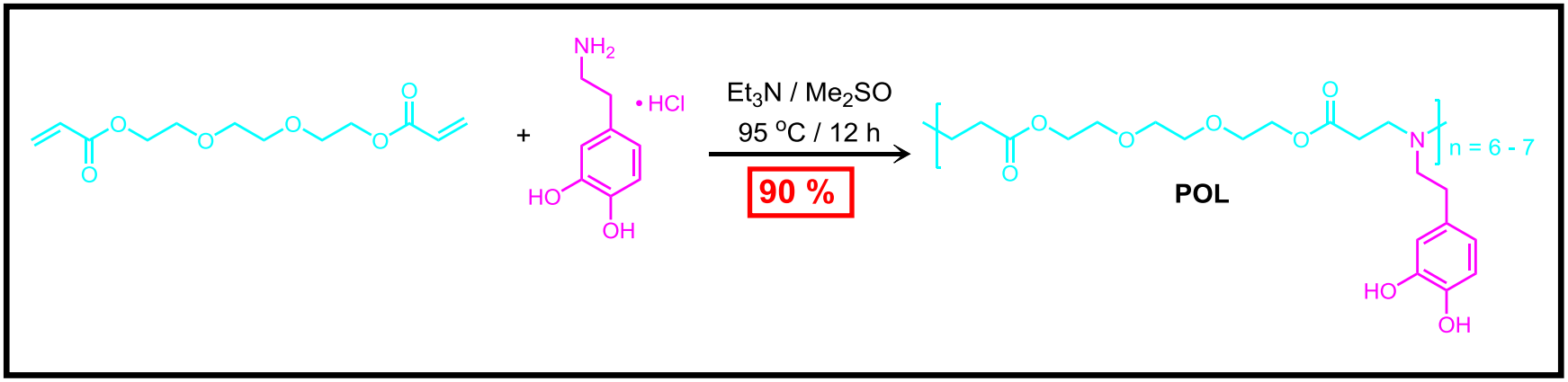

Fig. 2

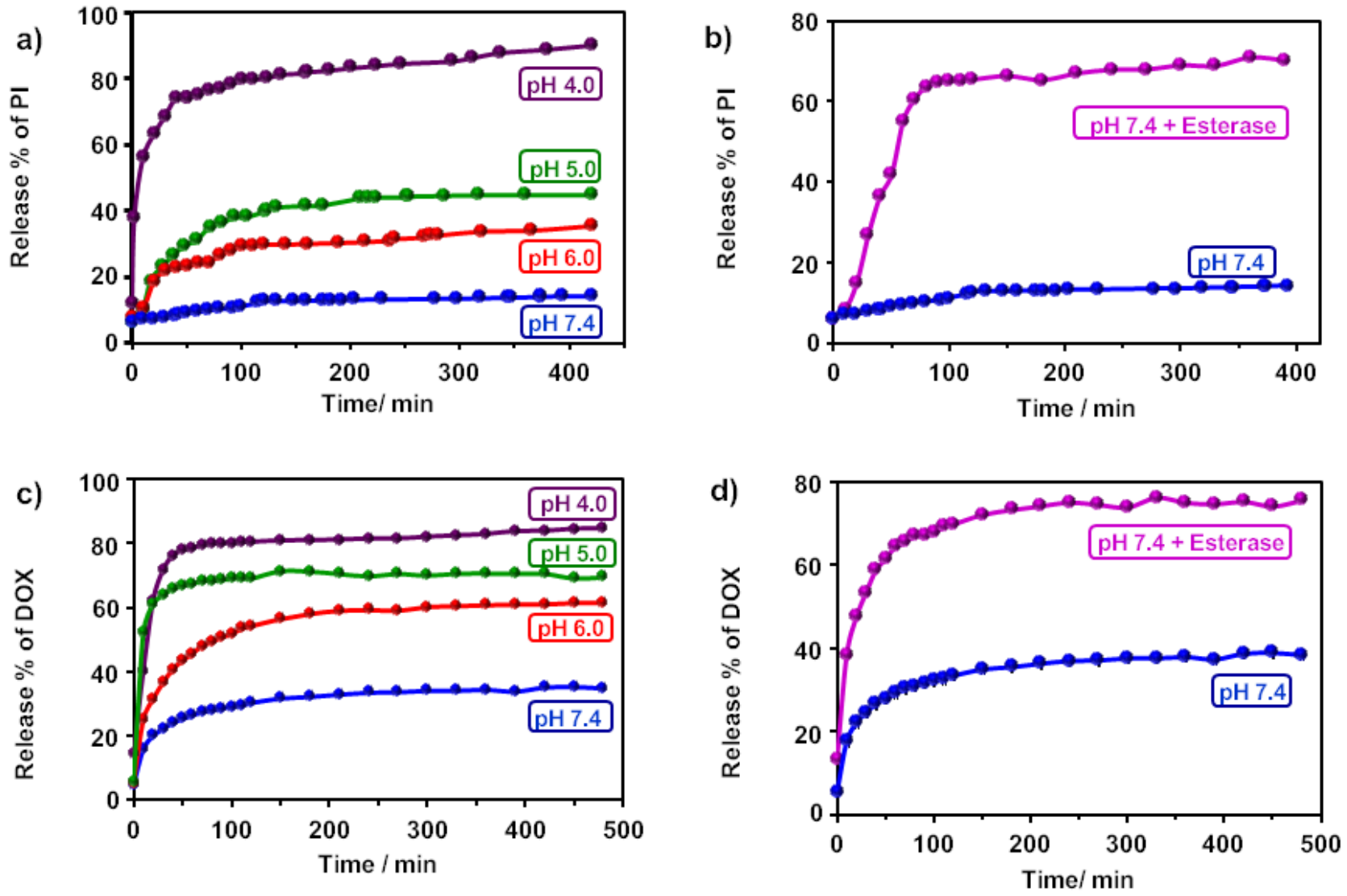
a)
Release % of PI
Time/ min
pH 4.0
pH 5.0
pH 6.0
pH 7.4
b)
Release % of PI
Time / min
pH 7.4 + Esterase
pH 7.4
c)
Release % of DOX
Time / min
pH 4.0
pH 5.0
pH 6.0
pH 7.4
d)
Release % of DOX
Time/ min
pH 7.4 + Esterase
pH 7.4

Fig. 3

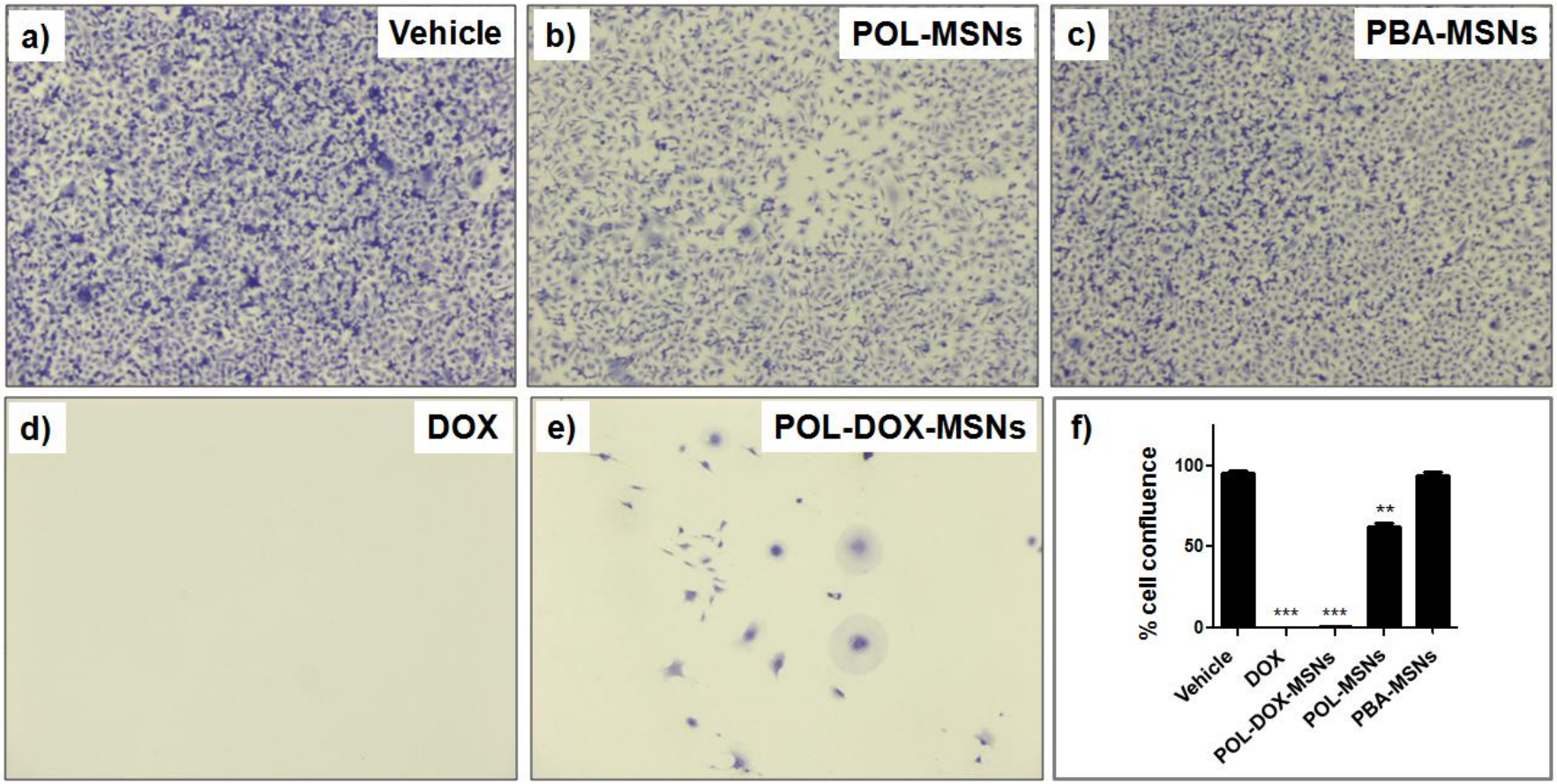
a)
Vehicle
b)
POL-MSNs
c)
PBA-MSNs
d)
DOX
e)
POL-DOX-MSNs
f)
% cell confluence
100
50
0
***
***
**
Vehicle
DOX
POL-DOX-MSNs
POL-MSNs
PBA-MSNs

Fig. 4